

FRACTAL STRUCTURE IN THE DIRECTED LANDSCAPE

SHIRSHENDU GANGULY AND MILIND HEGDE

ABSTRACT. This short article surveys recent progress in investigations of fractal structure in the directed landscape, which is a putative universal scaling limit within the KPZ universality class and a canonical example of random planar geometry.

Dedicated to Professor Rajeeva L. Karandikar on his 65th birthday.

1. INTRODUCTION

A broad area of much recent research in probability, pursued in several distinct directions, is *random geometry* and *random metric spaces*, with much of the focus on the planar case (planarity in fact plays an important role). The objects of interest include distance minimizing paths—*geodesics*—as well as the metric itself. The underlying disorder leads to certain key differences from standard models of geometry, such as those arising from Euclidean spaces, some of which will play central roles in the remainder of this article.

Most of these models are expected to exhibit certain approximate scale invariance features which should become exact once an appropriate limit is taken. Such invariance properties often manifest themselves in intricate *fractal behaviour*, the topic reviewed in this article. For the uninitiated reader, this essentially refers to various patterns of self-similarity ubiquitous in nature [[HNCS22a](#), [HNCS22b](#)]. While this survey covers rather modern developments, the general theme is a fairly familiar story in probability theory, where, for example, a similar line of consequences arises in Brownian motion, a universal scaling limit of one dimensional stochastic process; except that we are now dealing with significantly more complex high-dimensional random objects. At first glance, mathematical analysis of such properties may seem a daunting task. Nonetheless, there have been quite a few recent developments, and it turns out that many parallels and inspirations can be drawn from results about Brownian motion.

There are two broad classes of models of random planar geometry that have featured in most of the investigations. A first choice might be to choose a metric in some sense uniformly (with the base space fixed). Though highly nontrivial, this can indeed be made sense of. However, in this article we will consider a seemingly much simpler class of models which nevertheless leads to an equally rich theory. Perhaps the easiest example in this class consists of distorting the edge lengths in the Euclidean lattice by random weights. In other words, each edge is assigned an i.i.d. non-negative random variable which is its new length. Then the resulting graph metric is a random metric. This class of models, which is known as first passage percolation (FPP) was first introduced by

SHIRSHENDU GANGULY, DEPARTMENT OF STATISTICS, U.C. BERKELEY, BERKELEY, CA, USA

MILIND HEGDE, DEPARTMENT OF MATHEMATICS, COLUMBIA UNIVERSITY, NEW YORK, NY, USA

E-mail addresses: sganguly@berkeley.edu, milind.hegde@columbia.edu.

SG is partially supported by NSF grant DMS-1855688, NSF CAREER Award DMS-1945172 and a Sloan Research Fellowship. MH is partially supported by NSF grant DMS-1937254.

Hammersley and Welsh to model fluid flow in a porous medium [HW65]; the interested reader is encouraged to look at the survey [ADH17].

It is worth remarking that while in the above example the underlying noise that drives the randomness is independent, the earlier mentioned example of a “uniform” metric corresponds to a logarithmically correlated noise field. The central object of study in this direction is known as Liouville quantum gravity, for which there are many recent surveys available; we point the reader to [Gwy19, DDG21].

The case of interest for us, where the noise is independent (in fact, i.i.d.) falls into the Kardar-Parisi-Zhang universality class, a class of stochastic growth models (with the metric balls modeling growth) which are all believed to exhibit universal behaviour (akin to the universality of the central limit theorem). However, as alluded to earlier, we will be concerned with recent advances in understanding the geometric and fractal properties of some purportedly universal limiting objects, rather than aspects of universality itself.

1.1. Fractality in Brownian motion. Before turning to fractal behaviour in the aforementioned more complex settings, to offer a flavor of the kind of results we will be interested in, we start by recalling an abridged history of fractal properties in (one-dimensional) Brownian motion. The first and perhaps most classical instance of fractality usually encountered is that of its zero set: it is a perfect (closed, with no isolated points) set whose Hausdorff dimension (a heuristic definition is given in Section 3) is almost surely $\frac{1}{2}$. The basic fact that allows fractal behaviour to arise is that B is a stochastic process whose index set (i.e., its domain $[0, \infty)$, representing time) is *uncountable*. Thus, events which have probability zero at any fixed time (eg., $\mathbb{P}(B(t) = 0) = 0$ for any fixed $t > 0$) can nevertheless arise at a random exceptional time; the one-point probability estimate can only be extended to cover a countable set of times by a union bound, but cannot cover the entire domain. In all of the examples of fractality we will encounter in random metric spaces, this basic mechanism will be at play: events which almost surely do not occur at any typical location will almost surely happen at random exceptional locations, and the set of these exceptional locations will be fractal.

A second interesting point is that the fractal properties of the random set of exceptional locations will often be *deterministic*, just as the Hausdorff dimension of the Brownian zero set is deterministically $\frac{1}{2}$ almost surely. This can be understood as the manifestation of a kind of zero-one law which results from the approximate independence of these stochastic processes across different scales. After all, the question of fractal structure of these sets is exactly a question of the behaviour of the process across all small scales.

While one can formulate approximate statements for discrete random walks, ultimately fractal properties exist in a direct sense only in Brownian motion, their scaling limit. Similarly while there are many discrete models of random planar metric spaces with i.i.d. noise, such as FPP above, we will need a continuum object to investigate fractal properties. This is described in the next section. (It is worth pointing out that beyond the focus of this article on geodesic geometry, fractal properties have also been investigated in closely related models in the KPZ class in a number of recent studies, for example [CHHM21, Dau22, SS21, Das22, DG21], but in view of brevity we do not discuss these here).

2. THE DIRECTED LANDSCAPE

While we started our discussion with a model of a random metric space, most of the results are in fact about a related variant which is directed, and admits remarkable “integrable” properties allowing access to algebraic inputs. This is in contrast to the general intractableness of FPP. These directed models go by the name of last passage percolation (LPP) where instead of length minimizing paths as in FPP, one considers directed length maximizing paths (which are usually termed as geodesics as well). The scaling limit in this setting is what we will work with, which as a consequence of the

above, already has an in-built direction, and is called the *directed landscape*, first constructed in the breakthrough paper [DOV22].

The directed landscape $\mathcal{L} : \mathbb{R}_\dagger^4 \rightarrow \mathbb{R}$ is a random continuous function, where $\mathbb{R}_\dagger^4 = \{(x, s; y, t) : x, y \in \mathbb{R}, 0 \leq s < t < \infty\}$; we will think of (x, s) and (y, t) as pairs of points, and $\mathcal{L}(x, s; y, t)$ as a sort of “distance” between such points. That we require $s \leq t$ is a manifestation of the already alluded to the directedness in the models expected to converge to \mathcal{L} . Further, \mathcal{L} satisfies the reverse triangle inequality owing to the length maximization property: for $(p; r), (q; r), (p; q) \in \mathbb{R}_\dagger^4$,

$$\mathcal{L}(p; r) \geq \mathcal{L}(p; q) + \mathcal{L}(q; r).$$

In fact, this follows from a *metric composition* law that \mathcal{L} possesses: for $(x, r; z, t) \in \mathbb{R}_\dagger^4$ and any $s \in (r, t)$,

$$\mathcal{L}(x, r; z, t) = \max_{y \in \mathbb{R}} \mathcal{L}(x, r; y, s) + \mathcal{L}(y, s; z, t).$$

We should emphasize that there are currently only a handful of LPP models which can be shown to converge in some sense to the directed landscape.

As one would expect of any object which is a universal scaling limit (think again of Brownian motion), \mathcal{L} possesses a scale invariance property as well as many symmetries, governed by the now well-known KPZ scaling exponents of $\frac{1}{3}$ and $\frac{2}{3}$, where $\frac{1}{3}$ describes the length fluctuation scale and $\frac{2}{3}$ the spatial correlation scale. The precise statement of scale invariance (along with a convenient translation invariance) is that, for fixed $t, s > 0$ and as a process in $x, y \in \mathbb{R}$,

$$\mathcal{L}(x, t; y, t + s) \stackrel{d}{=} s^{-1/3} \mathcal{L}(xs^{-2/3}, 0; ys^{-2/3}, 1).$$

The $\frac{1}{3}$ and $\frac{2}{3}$ should be contrasted with the scaling exponent of $\frac{1}{2}$ in the Gaussian universality class (we note in passing that $\frac{2}{3} = 1 - \frac{1}{3}$, while $\frac{1}{2} = 1 - \frac{1}{2}$, as a sort of very heuristic reason for why there are two exponents instead of one in the KPZ class). These scaling exponents will largely determine the values of fractal dimensions of various random exceptional sets we will consider.

2.1. Geodesics in \mathcal{L} . While the existence of geodesics is usually straightforward to show in the pre-limiting models, it is not a priori obvious that this property persists in the limit, i.e., that \mathcal{L} is a geodesic space. Further, note that the definition of \mathcal{L} does not explicitly contain an underlying noise field (unlike in the prelimit where the noise was i.i.d.). For this reason, the length (which we will also often refer to as weight, in keeping with common terminology in the literature) $\|\pi\|_{\mathcal{L}}$ of a continuous path $\pi : [s, t] \rightarrow \mathbb{R}$ under \mathcal{L} is defined as

$$\|\pi\|_{\mathcal{L}} = \inf_{k \in \mathbb{N}} \inf_{s=t_0 < t_1 < \dots < t_k=t} \sum_{i=1}^k \mathcal{L}(\pi(t_{i-1}), t_{i-1}; \pi(t_i), t_i).$$

Given the above, a path $\pi : [s, t] \rightarrow \mathbb{R}$ is said to be a *geodesic* from $(\pi(s), s)$ to $(\pi(t), t)$ if $\|\pi\|_{\mathcal{L}} = \mathcal{L}(\pi(s), s; \pi(t), t)$.

It is a non-trivial fact, proved in [DOV22], that, almost surely, geodesics exist between all pairs of points and that, almost surely for any given pair of points, the geodesic is unique.

One aspect of understanding the random geometry of \mathcal{L} is the joint behaviour of multiple geodesics between different end points. The simplest, of course, is the case of two geodesics. Let us start with an easy consequence of planarity.

Let p_ℓ, p_r, q be three points such that $(p_\ell; q), (p_r; q) \in \mathbb{R}_\dagger^4$ and p_ℓ is to the left of p_r (see the left panel of Figure 1). Let γ_ℓ and γ_r respectively be the geodesics from p_ℓ and p_r to q . We work on the probability one event where these geodesics are unique. We claim that γ_ℓ is to the left of γ_r , i.e., $\gamma_\ell(s) \leq \gamma_r(s)$ for any s which belongs to the domains of both paths; in particular, while the two can touch, they cannot cross. We will refer to this as the *ordering* of geodesics.

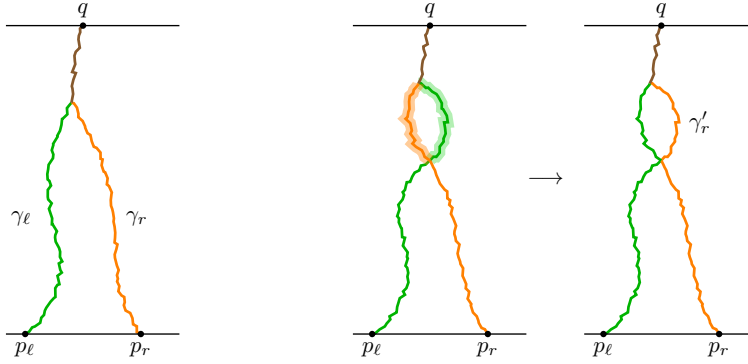


FIGURE 1. In the left panel we see that a geodesic γ_ℓ whose endpoints are to the left of that of another γ_r will lie to the left of it for its entire journey; the two geodesics may, however, coincide. This is known as geodesic ordering. The right panel depicts the argument for this ordering: if it did not hold and γ_ℓ crossed over γ_r , then a “bubble” would be formed between the two geodesics. Then we can construct new geodesics γ'_ℓ and γ'_r (between the same respective endpoints as the originals) by swapping which geodesic each of the sides of the bubble belong to, as shown. This contradicts the almost sure uniqueness of geodesics between fixed endpoints.

The proof is simple. Suppose γ_r crosses over γ_ℓ at some height. Because the paths are continuous and because of the ordering of the endpoints (along with planarity), γ_r must touch γ_ℓ at some later height. Look at both geodesics on the vertical interval between these two heights; it consists of two paths *with the same endpoints*; see the right panel of Figure 1. The left path is a subset of γ_r while the right is a subset of γ_ℓ . Because both geodesics are length maximizers, the left and right paths must have the same lengths. Because they share the same endpoints on this interval, we can define a new path γ'_r which equals γ_r except in between the two heights, where it equals the *right* path—in short, we have swapped the two paths on the mentioned interval of heights. Then γ'_r is a path with the same endpoints and the same length as γ_r , which means γ'_r is also a geodesic, which contradicts the uniqueness of γ_r .

So we know that geodesic whose endpoints are ordered cannot cross—but they can touch. What is the structure of this touching? Reviewing the above argument more closely shows that, again on the almost sure event that the two geodesics are unique, the set of heights where the two geodesics touch must be an interval; if not, we would again have a “bubble” which could be used to create distinct geodesics by a swapping operation; this observation applies even if the endpoints are not ordered. Thus, if two geodesics meet at some point, they will remain together for some interval of time, before separating and never meeting again (or they may never separate, if they have a common destination). This is called *geodesic coalescence*, induced by the propensity of the geodesics to pass through the atypically large part of environment, a key distinction from Euclidean geometry where geodesics are straight lines and hence have trivial intersection patterns.

3. GEODESIC COALESCENCE IN \mathcal{L}

Instead of directly trying to understand geodesic coalescence in full, it will prove fruitful to consider what can be thought of as a lower dimensional projection. Concretely, we focus on the case where geodesic have fixed distinct starting points, say $(-1, 0)$ and $(1, 0)$, and a common ending point $(x, 1)$. Because the geodesic certainly meet at height 1, it follows from the above discussion that the set of times where they meet must be an interval $[y_x, 1]$ (that the interval is closed follows from the continuity of the paths). It can be shown that, for any given $x \in \mathbb{R}$, with probability 1, $y_x < 1$, i.e., there is a non-trivial interval of coalescence. Therefore, it is natural to ask if there exist random

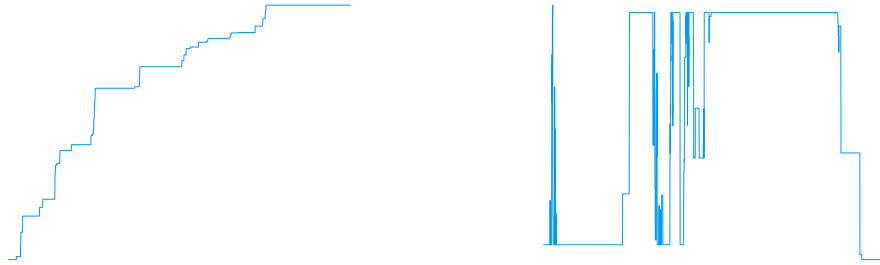


FIGURE 2. In the left panel we have a simulation of $x \mapsto \mathcal{D}(x, 1)$, while on the right it is $t \mapsto \mathcal{D}(0, t)$. Note that the left process is non-decreasing, while the right one does not exhibit any monotonicity. Both simulations are done in the discrete model of Exponential last passage percolation, which is known to converge to \mathcal{L} .

exceptional values of x where $y_x = 1$, i.e., endpoints such that the geodesics remain disjoint for their entire lifetimes except for the final instant? We will say that such geodesics are disjoint, ignoring the shared final point.

Much of the information pertaining to the above question turns out to be encoded by a projection of \mathcal{L} called the *weight difference profile* $\mathcal{D} : \mathbb{R} \times (0, \infty) \rightarrow \mathbb{R}$ by

$$\mathcal{D}(x, t) = \mathcal{L}(1, 0; x, t) - \mathcal{L}(-1, 0; x, t).$$

This object (in fact, only its spatial marginal $x \mapsto \mathcal{D}(x, 1)$, which we will denote \mathcal{D}_{sp}) was first introduced in [BGH21]. The expert reader might notice that this is closely related to, and can be thought of as a finite version of, *Busemann functions* from differential geometry which indeed have proven to be a valuable tool in studying FPP [Hof08].

It was shown in [BGH21, BGH22] that if x is such that the geodesics from $(-1, 0)$ and $(1, 0)$ to $(x, 1)$ are not disjoint, then \mathcal{D}_{sp} is constant in some neighbourhood of x . Thus, the fact that any fixed x is almost surely such that the mentioned geodesics are not disjoint implies that \mathcal{D}_{sp} is almost everywhere locally constant. Because the proofs of these statements rely only on geodesic coalescence, they also hold for the full process $(x, t) \mapsto \mathcal{D}(x, t)$ (the formal statement appears in the later article [GZ22]).

A curious fact, which is also a reasonably straightforward consequence of planarity, is that \mathcal{D}_{sp} is non-decreasing. Thus \mathcal{D}_{sp} is a random version of Cantor's function: almost everywhere constant, but nevertheless steadily increasing (a computation involving \mathcal{L} shows that the growth rate is on average linear). (This statement does not hold for the full process, eg. for $t \mapsto \mathcal{D}(0, t)$, which will cause complications in the latter's study; we will discuss this a bit more later.) See Figure 2.

The fact that the function is almost everywhere locally constant implies that the Lebesgue measure of the set of points of *non-constancy* (points where the function is not constant in any neighbourhood) is zero. A finer notion is needed to measure the size of these sets. A common choice is that of *fractal dimension*. While there are several definitions of fractal dimension available, a robust notion is the Hausdorff dimension. We do not include the somewhat technical definition, but remark that for purposes of intuition it is useful to keep in mind that the dimension of a subset $X \subseteq \mathbb{R}^n$ can be thought of the related number $\alpha > 0$ such that order $\varepsilon^{-\alpha}$ number of balls of radius ε are needed to cover X . For example, the Hausdorff dimension of a non-trivial interval is 1, of the unit square is 2, and so on.

It is well-known that the fractal dimension of the classical Cantor set, the set of points of non-constancy of the Cantor function, is $\log 2 / \log 3$. The main result of [BGH21] determined the fractal dimension of the set of non-constancy points of \mathcal{D}_{sp} , which we will denote $\text{NC}(\mathcal{D}_{\text{sp}})$.

Theorem 3.1 (Theorem 1.1 of [BGH21]). *The Hausdorff dimension of $\text{NC}(\mathcal{D}_{\text{sp}})$ is almost surely $\frac{1}{2}$.*

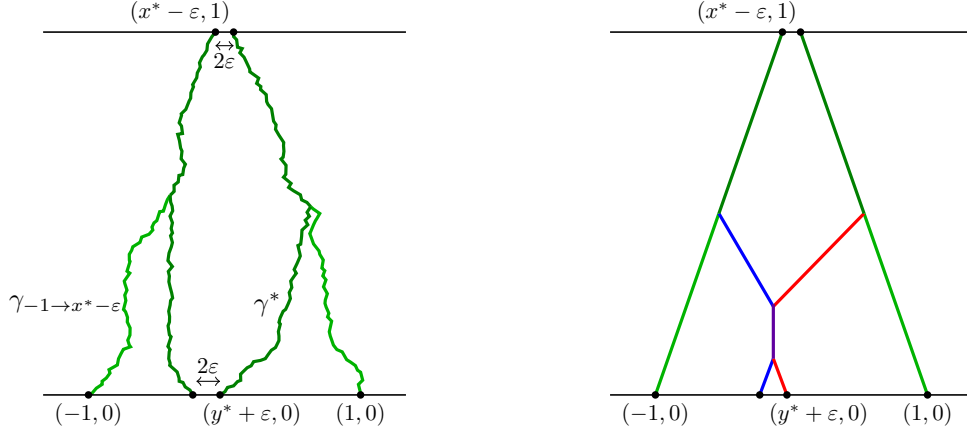


FIGURE 3. In the left panel we depict objects such as $\gamma_{-1 \rightarrow x^* - \varepsilon}$ and γ^* . Recall that y^* is the left-most point on the bottom such that the geodesic from $(y^*, 0)$ to $(x^* + \varepsilon, 1)$ is disjoint from $\gamma_{-1 \rightarrow x^* - \varepsilon}$. In the right panel we consider the case that the path formed by blue+purple+blue+dark green when going bottom to top and γ^* (red+purple+red+dark green) are not disjoint, and derive a contradiction. It is immediate from the diagram that we can then construct a new path γ' from $(y^* - \varepsilon, 0)$ to $(x^* + \varepsilon, 1)$ given by blue+purple+red+dark green; this is a geodesic since each of the path fragments making it up are portions of geodesics. Further, γ' is disjoint from $\gamma_{-1 \rightarrow x^* - \varepsilon}$ because the blue and purple path fragments in the figure are part of a geodesic which coalesces with the latter geodesic only later. So we have a geodesic from $(y^* - \varepsilon, 0)$ to $(x^* + \varepsilon, 1)$ which is disjoint from $\gamma_{-1 \rightarrow x^* - \varepsilon}$, contradicting our definition of y^* .

Let us now illustrate some of the ideas in [BGH21]’s proof of Theorem 3.1. As is usual while computing dimensions, one needs separate arguments for an upper bound and a lower bound on $\dim(\text{NC}(\mathcal{D}_{\text{sp}}))$.

The upper bound. For the upper bound, we use the earlier mentioned fact that $\text{NC}(\mathcal{D}_{\text{sp}})$ is a subset of the set Disj of x such that the two geodesics from $(-1, 0)$ and $(1, 0)$ to $(x, 1)$ are disjoint. (In fact, it was later shown in [BGH22] that the two sets coincide.) So it is enough to upper bound $\dim(\text{Disj})$.

There are multiple broadly similar arguments to show this, but here we outline a perhaps more geometric strategy. Suppose there is a random $x^* \in \text{Disj}$ (recall that any fixed $x \notin \text{Disj}$ a.s.), i.e., there are two disjoint geodesics from $(-1, 0)$ and $(1, 0)$ to $(x^*, 1)$. We claim that there must then be a random $y^* \in (-1, 1)$ such that there are *two* disjoint geodesics with endpoints in the intervals $[y^* - \varepsilon, y^* + \varepsilon] \times \{0\}$ and $[x^* - \varepsilon, x^* + \varepsilon] \times \{1\}$ —so two distinct geodesics between arbitrarily close endpoints.

The argument essentially is a consequence of planar ordering of geodesics. Consider the family of geodesics ending at $(x^* - \varepsilon, 1)$ (which is now fixed) indexed by the starting point $(y, 0)$ as y varies. Picture dragging the starting point y from -1 rightwards and observing how the geodesic to $(x^* + \varepsilon, 1)$ changes. There must be some smallest y^* at which the latter geodesic first becomes disjoint from the initial geodesic $\gamma_{-1 \rightarrow x^* - \varepsilon}$ from $(-1, 0)$. Let γ^* be the label of this geodesic from $(y^*, 0)$ to $(x^* + \varepsilon, 1)$ which is disjoint from $\gamma_{-1 \rightarrow x^* - \varepsilon}$. It can then be shown that the geodesics from $(y^* \pm \varepsilon, 0)$ to $(x^* \pm \varepsilon, 1)$ are disjoint (assuming the geodesic mentioned are unique, which can be ensured by looking at endpoints on a deterministic fine mesh). We give some more details in the caption of Figure 3.

So, given $x^* \in \text{Disj}$, we have found two disjoint geodesics whose endpoints are within ε of each other. It turns out, somewhat remarkably, that probability of such non-coalescence can be computed. In

fact, it was proved in [Ham20] that, given two intervals I_1 and I_2 of length ε , the probability that there are two disjoint geodesics with endpoints in $I_1 \times 0$ and $I_2 \times 1$ is at most of order $\varepsilon^{3/2}$; let us call this event E_{I_1, I_2} . With this result in hand, let us divide up the horizontal line segments (of some fixed finite width at least 2, so that ± 1 are contained in them) at heights 0 and 1 into intervals of length ε . There are $O(\varepsilon^{-1})$ many such intervals on each line segment, so $O(\varepsilon^{-2})$ many pairs of intervals, one taken from each of the two line segments.

We know from the argument above that for any ε -interval I_1 on the upper segment that contains x^* , there is an ε -interval I_2 on the lower line segment such that E_{I_1, I_2} occurs. By the result from [Ham20], the expected number of pairs of such intervals is at most $\varepsilon^{-2} \times \varepsilon^{3/2} = \varepsilon^{-1/2}$. Thus the number of ε -intervals that contain a point like x^* is also at most $\varepsilon^{-1/2}$. This yields a Hausdorff dimension upper bound of $\frac{1}{2}$.

The lower bound. Generally, it is harder to give a lower bound on the Hausdorff dimension of a set than an upper bound. But here, surprisingly, a matching lower bound is easier to obtain, albeit relying on some key properties of the landscape. To outline it, we need to introduce a related process known as the parabolic Airy₂ process \mathcal{P}_1 (the reason for the subscript of 1 will be made clear in a few more pages): it can be defined as $\mathcal{P}_1(x) = \mathcal{L}(0, 0; x, 1)$, i.e., the weight profile in the directed landscape as a function of the varying ending point when the starting point is fixed.

Here the important fact about \mathcal{P}_1 is that it is *locally Brownian*. There are many ways in which this vague statement can be made precise (see for example [CHH22, CH14, Ham22]), but the one relevant here is that \mathcal{P}_1 is Hölder- $\frac{1}{2}^-$ [Ham19]. As a result, \mathcal{P}_1 can vary over an interval of size ε by order $\varepsilon^{1/2}$.

Now $\mathcal{D}_{\text{sp}}(x) = \mathcal{L}(1, 0; x, 1) - \mathcal{L}(-1, 0; x, 1)$ can be regarded as the difference of a pair of coupled copies of \mathcal{P}_1 using the translation invariance of \mathcal{L} . Thus it too can vary over an interval of size ε by at most order $\varepsilon^{1/2}$.

The idea now is to divide up a given interval, say $[-1, 1]$, into sub-intervals of length ε^{-1} and ask for a lower bound on the number of these subintervals which contain a point of $\text{NC}(\mathcal{D}_{\text{sp}})$, i.e., a point where \mathcal{D}_{sp} increases. But since $\mathcal{D}_{\text{sp}}(1) - \mathcal{D}_{\text{sp}}(-1)$ is a unit order quantity, the control on the growth of \mathcal{D}_{sp} from above implies that at least order $\varepsilon^{-1/2}$ many intervals are needed to obtain $O(1) = O(\varepsilon^{1/2} \times \varepsilon^{-1/2})$ growth. This yields the matching lower bound of $\frac{1}{2}$ for $\dim(\text{NC}(\mathcal{D}_{\text{sp}}))$.

Note the crucial fact that \mathcal{D}_{sp} is monotone, and so an increase in one of the sub-intervals can only add to and not cancel that in another. As mentioned, this feature will not be present when we look at the related situation of the temporal slice of \mathcal{D} later.

3.1. The weight difference profile and Brownian local time. With Theorem 3.1 stating that $\text{NC}(\mathcal{D}_{\text{sp}})$ is a random fractal set of Hausdorff dimension $1/2$, one is naturally reminded of the already alluded to zero set of Brownian motion, i.e., $\{t > 0 : B(t) = 0\}$ where B is a standard Brownian motion started at 0 (see for example [MP10, Theorem 4.24]). Associated is a natural stochastic process which is non-decreasing, almost everywhere constant, and whose points of non-constancy are exactly the Brownian motion zero set: the Brownian local time \mathfrak{L} . It can be thought of as a measure of the amount of time B spends at zero, and can be precisely defined using this intuition:

$$\mathfrak{L}(t) = \lim_{\varepsilon \downarrow 0} \frac{1}{2\varepsilon} \int_0^t \mathbb{1}_{B(s) \in [-\varepsilon, \varepsilon]} ds.$$

Amazingly, an identity of Lévy says that the local time has the same distribution as the running maximum process of Brownian motion. More precisely, if $M(t) = \sup_{0 \leq s \leq t} B(s)$, then, as processes,

$$\mathfrak{L} \stackrel{d}{=} M.$$

Now, because \mathfrak{L} is non-negative and non-decreasing, it can be interpreted as the distribution function of a probability measure supported on the zero set of Brownian motion. A well-known technique to understand the Hausdorff dimension of a set is to construct a measure on it with certain mass distribution properties, and the argument for the Hausdorff dimension of the zero set of Brownian motion uses the measure defined via \mathfrak{L} , along with the distributional identity of \mathfrak{L} with M for the analysis of the measure.

All of the above leads to an obvious question: is there a connection between \mathcal{D} and \mathfrak{L} ? It turns out that indeed there is.

Theorem 3.2 ([GH22, Dau21]). *Let $[a, b] \subseteq \mathbb{R}$. Then the law of $\mathcal{D}_{\text{sp}}(\cdot) - \mathcal{D}_{\text{sp}}(a)|_{[a, b]}$ is absolutely continuous to that of $\mathfrak{L}(\cdot) - \mathfrak{L}(1)|_{1, b-a+1}$.*

We need to consider the increment of \mathcal{D} as the process is not non-negative by itself (unlike \mathfrak{L}), and we consider \mathfrak{L} from the point 1 onward instead of zero because \mathfrak{L} increases almost surely at 0, but \mathcal{D} almost surely is locally constant at any fixed point.

Note that the Hausdorff dimension result of Theorem 3.1 is an immediate corollary of the just stated theorem, using the fact that the zero set of Brownian motion is almost surely $\frac{1}{2}$.

Theorem 3.2 is a global comparison in the sense that we consider the process on a unit order interval. One can also do a local comparison, in which we focus on the process in a neighborhood of a given point. For appropriate choice of (random) point, one obtains Brownian local time *exactly*, unlike the absolute continuity type of comparison made in Theorem 3.2.

More precisely, by a local comparison, we mean distributional limits of the form $\varepsilon^{-1/2}(\mathcal{D}_{\text{sp}}(\tau + \varepsilon t) - \mathcal{D}_{\text{sp}}(\tau))$ where τ is a random time. First, note that τ indeed needs to be random: at a deterministic time, \mathcal{D}_{sp} is almost surely locally constant, and so the local limit will be trivial. Further, for the same reason, τ needs to be almost surely a point of increase of \mathcal{D}_{sp} (i.e., τ is such that $\mathcal{D}_{\text{sp}}(\tau + \varepsilon) > \mathcal{D}_{\text{sp}}(\tau)$ for every $\varepsilon > 0$) for there to be any hope of obtaining \mathfrak{L} in the limit.

Now, there are a number of ways of choosing a point of increase of \mathcal{D}_{sp} . For instance, we may fix $\lambda \in \mathbb{R}$ and consider the first point of increase τ_λ following λ . This would, in some sense, be a choice size-biased by the length of the flat portion preceding τ_λ ; also, it excludes any of the “interior” points of increase of \mathcal{D}_{sp} from being considered. Alternately, we could choose, for an interval $[c, d]$, a point $\xi_{[c, d]}$ *uniformly* from all the non-constant points of \mathcal{D}_{sp} on $[c, d]$, by sampling from the probability measure on $[c, d]$ with distribution function $(\mathcal{D}_{\text{sp}}(\cdot) - \mathcal{D}_{\text{sp}}(c))/(\mathcal{D}_{\text{sp}}(d) - \mathcal{D}_{\text{sp}}(c))$, conditionally on the event that this is a non-zero measure (which is shown to hold with positive probability in [GH22]). (Indeed, distributions at random times sampled according to such local times have been studied, for example, in the context of dynamical critical percolation [HPS15].)

The local limit at both these types of random times is Brownian local time:

Theorem 3.3 ([GH22]). *Let τ be equal to either τ_λ or $\xi_{[c, d]}$ (the second conditionally on $\text{NC}(\mathcal{D}_{\text{sp}}) \cap [c, d] \neq \emptyset$) as above. Then,*

$$\lim_{\varepsilon \rightarrow 0} \varepsilon^{-1/2} (\mathcal{D}_{\text{sp}}(\tau + \varepsilon t) - \mathcal{D}_{\text{sp}}(\tau)) = \mathfrak{L}(t),$$

where the limit is in distribution in the topology of uniform convergence on compact sets of $[0, \infty)$.

In fact there are a couple more random times for which Theorem 3.3 is proved in [GH22], such as the first time \mathcal{D}_{sp} hits a given deterministic level.

The arguments from [BGH21] provided no insight into the probabilistic structure of \mathcal{D}_{sp} such as that stated in the last two theorems, and hence the proofs of these take a rather different route. We sketch some key features.

First recall the parabolic Airy₂ process $\mathcal{P}_1(\cdot) = \mathcal{L}(0, 0; \cdot, 1)$ introduced above. An important line of research within KPZ over the last decade has relied on embedding \mathcal{P}_1 in an ensemble of an infinite

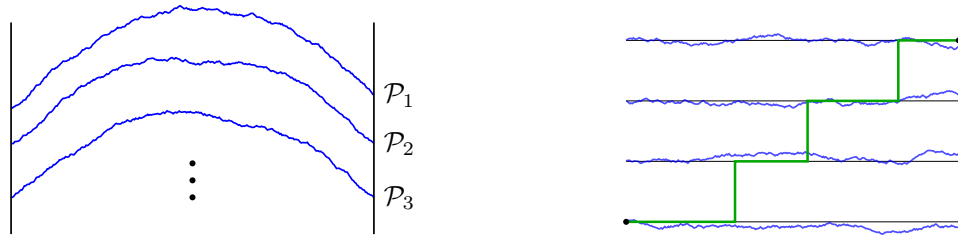


FIGURE 4. On the left is a depiction of the parabolic Airy_2 line ensemble \mathcal{P} . On the right is an example of an up-right path in an environment given by \mathcal{P} (shown without parabolic curvature for convenience).

collection of random, continuous, non-intersecting curves. This ensemble is known as the parabolic Airy line ensemble and is denoted \mathcal{P} ; \mathcal{P}_1 is the highest in terms of value as well as lowest-indexed curve in the ensemble. See Figure 4.

The ensemble was constructed in [CH14]. The important feature of \mathcal{P} , which is the reason it has proved a crucial tool within KPZ, is that it possesses an explicit resampling property in terms of non-intersecting Brownian bridges. This is known as the *Brownian Gibbs* property and it states the following for any fixed interval $[a, b]$ and $k \in \mathbb{N}$: the conditional distribution of $\mathcal{P}_1, \dots, \mathcal{P}_k$ on $[a, b]$, conditional on the data of $\mathcal{P}_1, \dots, \mathcal{P}_k$ outside $[a, b]$ and $\mathcal{P}_{k+1}, \mathcal{P}_{k+2}, \dots$ on all of \mathbb{R} , is given by k independent rate *two* Brownian bridges $B_1, \dots, B_k : [a, b] \rightarrow \mathbb{R}$, with $B_i(a) = \mathcal{P}_i(a)$ and $B_i(b) = \mathcal{P}_i(b)$, conditioned on not intersecting each other or the lower curve \mathcal{P}_{k+1} .

The curves below the top one in \mathcal{P} also have an interpretation via the Robinson-Schensted-Knuth (RSK) correspondence from algebraic combinatorics, which we will not get into, except mentioning that the latter is the key underlying device using which the earlier quoted estimate on the probability of non-coalescence was proven in [Ham20].

We will now state a rather remarkable and powerful statement which played a central role in the construction of the directed landscape \mathcal{L} in [DOV22]. This involves considering last passage percolation across an environment defined by the parabolic Airy line ensemble. Analogous to the definition of geodesics in \mathcal{L} , we will consider a class of paths which are directed, assign a weight to each path in terms of the environment, and maximize the weight over all paths between given points. The class of directed paths are up-right paths; see the right panel of Figure 4. An up-right path is assigned weight given by the summing the increments of \mathcal{P}_i along the path, i.e., is the path lies on line i on the interval $[a_i, b_i]$ for each i , then its weight is $\sum \mathcal{P}_i(b_i) - \mathcal{P}_i(a_i)$.

The above mentioned last passage problem in \mathcal{P} can be described by fixing a starting coordinate on the k^{th} line (for some $k \geq 1$) and an ending coordinate on the first (i.e., top) line, and considering up-right paths between the two. The weight of a given path is given by the sum (over i) of increments of values of \mathcal{P}_i along the interval that the path spends on the i^{th} line. If the starting point is (y, k) and ending point is $(x, 1)$, we denote this by $\mathcal{P}[(y, k) \rightarrow (x, 1)]$.

It was shown in [DOV22] that, roughly speaking, that $\mathcal{L}(0, y; x, 1)$ is equal to a certain last passage value in \mathcal{P} where the starting point can be thought to be at $-\infty$, but in a way that depends on y , and the ending points is x on the top curve \mathcal{P}_1 . This generalizes the earlier mentioned property that $\mathcal{L}(0, 0; x, 1) = \mathcal{P}_1(x)$ for all $x \in \mathbb{R}$, more precisely that there is a coupling between \mathcal{L} and \mathcal{P} such that that holds.

This basic representation of \mathcal{L} in terms of a last passage problem through \mathcal{P} is the underlying reason for the local time-like behaviour of \mathcal{D}_{sp} . More precisely, let us suppose that our two starting points for \mathcal{D}_{sp} are 0 and 1 instead of -1 and 1; this is useful because $\mathcal{L}(0, 0; x, 1) = \mathcal{P}_1(x)$. We can handle the general case using stationarity properties of \mathcal{L} . Then we can write $\mathcal{D}_{\text{sp}}(x) = \mathcal{L}(1, 0; x, 1) - \mathcal{L}(0, 0; x, 1)$

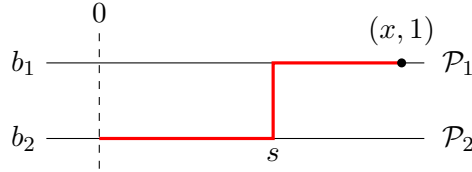


FIGURE 5. A depiction of the toy example discussed in the text, with $b_i = \mathcal{P}_i(0)$. The red line jumps at the location s where the maximization $\max_{0 \leq s \leq x} (\mathcal{P}_2(s) - \mathcal{P}_1(s))$ is achieved. In fact, one can think of the red line as a geodesic in the environment given by the parabolic Airy line ensemble \mathcal{P} .

as an infinite LPP problem in \mathcal{P} which ends at x on the top line, minus $\mathcal{P}_1(x)$. (This representation of \mathcal{L} as an infinite LPP problem in \mathcal{P} is made precise in [SV21].)

In this article, for simplicity, we assume a toy situation where we simply have two lines on the interval $[0, x]$ for some $x > 0$ and consider the LPP problem with two sources being $\{1, 2\} \times \{0\}$ pretending that they yield the values $\mathcal{L}(0, 0; x, 1)$ and $\mathcal{L}(1, 0; x, 1)$ respectively. (The argument in [GH22] proceeds by reducing the original problem essentially to the above problem.)

This means that we can write

$$\mathcal{L}(1, 0; x, 1) = b_2 + \mathcal{P}[(0, 2) \rightarrow (x, 1)] = b_2 + \max_{0 \leq s \leq x} [\mathcal{P}_1(x) - \mathcal{P}_1(s) + \mathcal{P}_2(s) - \mathcal{P}_2(0)].$$

where b_i is the value of \mathcal{P}_i at 0 for $i = 1, 2$. Since $\mathcal{L}(0, 0; x, 1) = \mathcal{P}_1(x)$, we get that

$$\mathcal{D}_{\text{sp}}(x) = b_2 + \max_{0 \leq s \leq x} [\mathcal{P}_2(s) - \mathcal{P}_1(s)] - \mathcal{P}_2(0).$$

Putting in $x = 0$ shows that $\mathcal{D}(0) = b_2 - \mathcal{P}_1(0)$, so that

$$\mathcal{D}_{\text{sp}}(x) - \mathcal{D}_{\text{sp}}(0) = \max_{0 \leq s \leq x} [(\mathcal{P}_2(s) - \mathcal{P}_2(0)) - (\mathcal{P}_1(s) - \mathcal{P}_1(0))].$$

We now see the reason for the appearance of Brownian local time: the increments of curves of \mathcal{P} are Brownian-like, in the sense that any finite collection on any compact interval are jointly absolutely continuous to independent rate two Brownian motions started from appropriate points, and the running maximum process of Brownian motion, by the identity of Lévy mentioned above, is exactly (in distribution) Brownian local time. The absolute continuity statement comparing \mathcal{P} to Brownian motion is an easy consequence of the Brownian Gibbs property; see [CH14, Corollary 4.3].

3.2. Geodesic local time. While Brownian local time encodes the time that Brownian motion spends at zero, given all the discussions so far, it is natural to wonder if a counterpart exists for the geodesics in \mathcal{L} which clearly forms another important class of random curves: for example, does there exist a process, a *geodesic local time*, which measures the amount of time that a geodesic spends at zero? Besides being an independently interesting object of study, it has several applications as we will briefly allude to.

The geodesic local time was constructed recently in [GZ22]. To discuss it more precisely, we need to introduce *semi-infinite geodesics*. Given a direction $r \in \mathbb{R}$, a semi-infinite geodesic from $(0, 0)$ in the direction r is a path $\pi_r : [0, \infty) \rightarrow \mathbb{R}$ such that (i) $t^{-1}\pi_r(t) \rightarrow r$ as $t \rightarrow \infty$ and (ii) for any $0 \leq s_1 < s_2 < \infty$, the restriction of π_r to $[s_1, s_2]$ is a geodesic from $(s_1, \pi_r(s_1))$ to $(s_2, \pi_r(s_2))$. See Figure 6.

Semi-infinite geodesics are objects of interest in both first passage and last passage percolation. A related concept is a bi-infinite geodesic, which is a path defined on all of \mathbb{R} instead of $[0, \infty)$ that shares the same property of all restrictions being geodesics. However, it is expected that (non-trivial) bi-infinite geodesics do not exist in first or last passage (non-trivial because in some models certain deterministic bi-infinite paths can be forced to satisfy the geodesic restriction property due to the

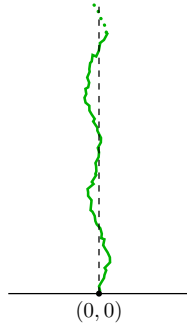


FIGURE 6. A depiction of the semi-infinite geodesic in the 0 direction (i.e., directly vertical) starting from $(0, 0)$.

definition of directed paths in the model), and this has been proven in certain integrable models of LPP [BHS18, BBS20] as well as in first passage percolation under some (unproven) hypotheses [DH17].

Thus the existence of semi-infinite geodesics is not immediate. They do exist, however (unlike what is believed about bi-infinite geodesics), and this has been proven in a number of models, including the directed landscape [GZ22, RV21, BSS22].

Let us consider the semi-infinite geodesic π_0 in the 0-direction. Analogous to \mathfrak{L} , we can search for a continuous stochastic process which is almost surely non-decreasing and whose points of non-constancy are exactly the times at which π_0 is at zero, i.e., the set of times $\{t > 0 : \pi_0(t) = 0\}$. This is the precise version of the geodesic local time we asked about above.

Theorem 3.4 ([GZ22]). *Almost surely, for every $t > 0$ simultaneously, the limit*

$$\lim_{\varepsilon \downarrow 0} \frac{1}{2\varepsilon} \int_0^t \mathbb{1}_{\pi_0(s) \in [-\varepsilon, \varepsilon]} ds$$

exists and is strictly positive.

In fact, it is further established in [GZ22] that the process is Hölder- $\frac{1}{3}^-$.

The proof of Theorem 3.4 proceeds differently compared to the construction of Brownian local time. This is necessitated by the basic fact that the underlying object of Brownian motion is a Markov process, while the semi-infinite geodesic π_0 is *not*; indeed, its value at any given height a priori depends on the entire infinite random environment.

Given the geodesic local time, one can try to understand the fractal structure of its set of points of non-constancy, analogous to finding the Hausdorff dimension of the zero set of Brownian motion using its local time.

Theorem 3.5 ([GZ22]). *The set $\{t > 0 : \pi_0(t) = 0\}$ almost surely has Hausdorff dimension $\frac{1}{3}$.*

The value of the dimension can be understood in terms of the continuity properties of π_0 . This is similar to how the fact that Brownian motion is Hölder- $\frac{1}{2}^-$ leads to the Hausdorff dimension of its zero set being $1 - \frac{1}{2} = \frac{1}{2}$. Geodesics in LPP have long been known to be Hölder- $\frac{2}{3}$ - [Joh00, HS20, DOV22], which suggests that the zero set of the geodesic should be expected to have Hausdorff dimension of $1 - \frac{2}{3} = \frac{1}{3}$ (note that these Hölder continuity results are for geodesics between deterministic points and so do not immediately transfer to semi-infinite geodesics, whose restrictions to finite intervals are only geodesics between random points).



FIGURE 7. A simulation of the full difference profile \mathcal{D} in a prelimiting model (Exponential LPP). Colours represent level sets. The strict colour gradation from left to right is a consequence of the monotonicity of the spatial marginal of \mathcal{D} , which, as can be seen by looking closely, is not present in the temporal direction.

3.3. The full spatio-temporal weight difference profile. The geodesic local time arose in [GZ22] in connection with another problem, that of understanding the fractal structure of the full difference profile process, i.e., which takes both spatial *and* temporal arguments.

As mentioned earlier, this two parameter weight difference profile shares the feature that it is almost everywhere constant with its spatial marginal that we have focused on thus far. However, unlike the spatial marginal, the temporal marginal $t \mapsto \mathcal{D}(x, t)$ for fixed $x \in \mathbb{R}$ is *not* monotone and the behavior is expected to be different; see Figure 7. Recently in this direction, [GZ22] established the following fractal dimension statements:

Theorem 3.6. *Fix $x \in \mathbb{R}$. The set of points of non-constancy of $t \mapsto \mathcal{D}(x, t)$ is almost surely equal to $\frac{2}{3}$.*

Note that the dimension is a more KPZ-esque multiple of $\frac{1}{3}$ rather than the Brownian-like $\frac{1}{2}$ for the spatial marginal. One can similarly ask for the fractal dimension of the non-constancy points of the entire spatio-temporal process:

Theorem 3.7. *The set of points of non-constancy of $(x, t) \mapsto \mathcal{D}(x, t)$ is almost surely equal to $\frac{5}{3}$.*

The arguments for the upper bounds of Theorems 3.6 and 3.7 are similar to the one for the upper bound in Theorem 3.1 via geometric considerations of geodesic disjointness. The lower bound, however, is much more difficult.

The basic problem is that, unlike in the spatial marginal of \mathcal{D} , the temporal and spatio-temporal versions are not monotone. Thus it is possible for the increment of \mathcal{D} that occurs in one ε -interval to be of the opposite sign as that in some other ε -interval, leading to some degree of cancellation. In fact, an argument similar to the one outlined for Theorem 3.1 using Hölder continuity properties of \mathcal{D} (this time in the temporal direction) would yield a lower bound of only $\frac{1}{3}$ in Theorem 3.6, precisely because cancellations have been ignored. Heuristically, this also explains why the true dimension is $\frac{2}{3}$: cancellations should follow a central limit theorem type effect, so that one expects the effective size after cancellations to be of order the square root of the sum of the absolute value of the increments; so to obtain the same overall change, if one needed $\varepsilon^{-1/3}$ many intervals to achieve a certain overall unit order increment when considering the sum of absolute values of the increments over ε -sub-intervals, then one should need $(\varepsilon^{-1/3})^2 = \varepsilon^{-2/3}$ many intervals after taking into account the cancellation effect, suggesting the true result of $\frac{2}{3}$.

3.4. Non-uniqueness of semi-infinite geodesics. The last topic we discuss in this survey concerns semi-infinite geodesics as introduced in the previous section. As we saw, we can define semi-infinite geodesics which go in the direction r for every $r \in \mathbb{R}$. We can also have the semi-infinite geodesics start from any point $p \in \mathbb{R}^2$ instead of just $(0, 0)$ in a completely analogous way.

It can be shown that semi-infinite geodesics exist in every direction and from every starting point simultaneously with probability one [BSS22] (it was previously shown in [RV21] that they almost surely exist in all directions for a fixed point, or for all points in a fixed direction).

Once we have existence, the question of uniqueness arises. For any fixed direction, there is a unique semi-infinite geodesic in that direction [RV21]; more precisely, semi-infinite geodesics which emanate from any starting point in that fixed direction will all ultimately coalesce into a single one.

The fact that this statement was made for each fixed direction immediately raises the possibility that there exist random exceptional directions in which there exist multiple semi-infinite geodesics which do not ultimately coalesce. In fact, [BSS22] showed that there is a random countable dense set Ξ of directions such that this happens. For each direction $\xi \in \Xi$ and $p \in \mathbb{R}^2$, there exist at least two semi-infinite geodesics starting at p in the direction ξ which separate at some point and never meet again; note that they need not be disjoint because of this possibly shared initial portion.

Because Ξ is countable, it does not possess any fractal structure. However, fractal structure is present if one fixes a random direction in Ξ and then considers the set of starting points $p = (x, s)$ such that there are at least two *disjoint* semi-infinite geodesics starting at p in that direction, which we call $\mathfrak{S}_\xi \subseteq \mathbb{R}^2$. [BSS22] studies the slice $\mathfrak{S}_{\xi,s}$ of this set where s is fixed:

Theorem 3.8. *For any fixed $s \in \mathbb{R}$, for every $\xi \in \Xi$, $\mathfrak{S}_{\xi,s}$ almost surely has Hausdorff dimension $\frac{1}{2}$.*

This theorem has close connections to Theorem 3.1; indeed, [BSS22] approaches this set via Busemann functions, which are closely related to the weight difference profile \mathcal{D} .

4. CONCLUSION

The study of fractal structure within the directed landscape has opened up many avenues of research, and introduced new probabilistic objects such as the geodesic local time which are not yet deeply understood. One broad direction to be explored is to continue a theme touched upon in this survey, namely to establish analogues of well-known properties of Brownian local time and its zero set for the geodesic local time and the set of heights when the semi-infinite geodesic is at zero. We similarly expect there to be a rich class of questions concerning other aspects of geodesic geometry that remain to be asked.

REFERENCES

- [ADH17] Antonio Auffinger, Michael Damron, and Jack Hanson. *50 years of first-passage percolation*, volume 68. American Mathematical Soc., 2017.
- [BBS20] Márton Balázs, Ofer Busani, and Timo Seppäläinen. Non-existence of bi-infinite geodesics in the exponential corner growth model. In *Forum of Mathematics, Sigma*, volume 8. Cambridge University Press, 2020.
- [BGH21] Riddhipratim Basu, Shirshendu Ganguly, and Alan Hammond. Fractal geometry of Airy₂ processes coupled via the Airy sheet. *The Annals of Probability*, 49(1):485–505, 2021.
- [BGH22] Erik Bates, Shirshendu Ganguly, and Alan Hammond. Hausdorff dimensions for shared endpoints of disjoint geodesics in the directed landscape. *Electronic Journal of Probability*, 27:1–44, 2022.
- [BHS18] Riddhipratim Basu, Christopher Hoffman, and Allan Sly. Nonexistence of bigeodesics in integrable models of last passage percolation. *arXiv preprint arXiv:1811.04908*, 2018.
- [BSS22] Ofer Busani, Timo Seppäläinen, and Evan Sorensen. The stationary horizon and semi-infinite geodesics in the directed landscape. *arXiv preprint arXiv:2203.13242*, 2022.
- [CH14] Ivan Corwin and Alan Hammond. Brownian Gibbs property for Airy line ensembles. *Inventiones mathematicae*, 195(2):441–508, 2014.

- [CHH22] Jacob Calvert, Alan Hammond, and Milind Hegde. Brownian structure in the KPZ fixed point. *Astérisque*, 2022+. To appear.
- [CHHM21] Ivan Corwin, Alan Hammond, Milind Hegde, and Konstantin Matetski. Exceptional times when the KPZ fixed point violates Johansson’s conjecture on maximizer uniqueness. *arXiv preprint arXiv:2101.04205*, 2021.
- [Das22] Sayan Das. Temporal increments of the KPZ equation with general initial data. *arXiv preprint arXiv:2203.00666*, 2022.
- [Dau21] Duncan Dauvergne. Last passage isometries for the directed landscape. *arXiv preprint arXiv:2106.07566*, 2021.
- [Dau22] Duncan Dauvergne. Non-uniqueness times for the maximizer of the KPZ fixed point. *arXiv preprint arXiv:2202.01700*, 2022.
- [DDG21] Jian Ding, Julien Dubedat, and Ewain Gwynne. Introduction to the Liouville quantum gravity metric. *arXiv preprint arXiv:2109.01252*, 2021.
- [DG21] Sayan Das and Promit Ghosal. Law of iterated logarithms and fractal properties of the KPZ equation. *arXiv preprint arXiv:2101.00730*, 2021.
- [DH17] Michael Damron and Jack Hanson. Bigeodesics in first-passage percolation. *Communications in Mathematical Physics*, 349(2):753–776, 2017.
- [DOV22] Duncan Dauvergne, Janosch Ortmann, and Bálint Virág. The directed landscape. *Acta Mathematica*, 2022+. To appear.
- [GH22] Shirshendu Ganguly and Milind Hegde. Local and global comparisons of the Airy difference profile to Brownian local time. *Ann. Inst. H. Poincaré Probab. Statist.*, 2022+. To appear.
- [Gwy19] Ewain Gwynne. Random surfaces and Liouville quantum gravity. *arXiv preprint arXiv:1908.05573*, 2019.
- [GZ22] Shirshendu Ganguly and Lingfu Zhang. Fractal geometry of the space-time difference profile in the directed landscape via construction of geodesic local times. *arXiv preprint arXiv:2204.01674*, 2022.
- [Ham19] Alan Hammond. Modulus of continuity of polymer weight profiles in Brownian last passage percolation. *The Annals of Probability*, 47(6):3911–3962, 2019.
- [Ham20] Alan Hammond. Exponents governing the rarity of disjoint polymers in Brownian last passage percolation. *Proceedings of the London Mathematical Society*, 120(3):370–433, 2020.
- [Ham22] Alan Hammond. Brownian regularity for the Airy line ensemble, and multi-polymer watermelons in Brownian last passage percolation. *Memoirs of the American Mathematical Society*, 277(1363), 2022.
- [HNCS22a] Akhlaq Husain, Manikyala Navaneeth Nanda, Movva Sitaram Chowdary, and Mohammad Sajid. Fractals: An eclectic survey, part I. *Fractal and Fractional*, 6(2):89, 2022.
- [HNCS22b] Akhlaq Husain, Manikyala Navaneeth Nanda, Movva Sitaram Chowdary, and Mohammad Sajid. Fractals: An eclectic survey, part II. *Fractal and Fractional*, 6(7):379, 2022.
- [Hof08] Christopher Hoffman. Geodesics in first passage percolation. *The Annals of Applied Probability*, 18(5):1944–1969, 2008.
- [HPS15] Alan Hammond, Gábor Pete, and Oded Schramm. Local time on the exceptional set of dynamical percolation and the incipient infinite cluster. *Annals of Probability*, 43(6):2949–3005, 2015.
- [HS20] Alan Hammond and Sourav Sarkar. Modulus of continuity for polymer fluctuations and weight profiles in Poissonian last passage percolation. *Electronic Journal of Probability*, 25:1–38, 2020.
- [HW65] John M Hammersley and Dominic JA Welsh. First-passage percolation, subadditive processes, stochastic networks, and generalized renewal theory. In *Bernoulli 1713, Bayes 1763, Laplace 1813*, pages 61–110. Springer, 1965.
- [Joh00] Kurt Johansson. Transversal fluctuations for increasing subsequences on the plane. *Probability theory and related fields*, 116(4):445–456, 2000.
- [MP10] Peter Mörters and Yuval Peres. *Brownian motion*, volume 30. Cambridge University Press, 2010.
- [RV21] Mustazee Rahman and Bálint Virág. Infinite geodesics, competition interfaces and the second class particle in the scaling limit. *arXiv preprint arXiv:2112.06849*, 2021.
- [SS21] Timo Seppäläinen and Evan Sorensen. Global structure of semi-infinite geodesics and competition interfaces in Brownian last-passage percolation. *arXiv preprint arXiv:2112.10729*, 2021.
- [SV21] Sourav Sarkar and Bálint Virág. Brownian absolute continuity of the KPZ fixed point with arbitrary initial condition. *The Annals of Probability*, 49(4):1718–1737, 2021.